Annals of Nuclear Energy 101 (2017) 36–48

Contents lists available at ScienceDirect

Annals of Nuclear Energy

journal homepage: www.elsevier.com/locate/anucene

Investigation on generalized Variational Nodal Methods for heterogeneous nodes

Yongping Wang [a], Hongchun Wu [a], Yunzhao Li [a,*], Liangzhi Cao [a], Wei Shen [a,b]

[a] School of Nuclear Science and Technology, Xi'an Jiaotong University, 28 West Xianning Road, Xi'an, Shaanxi 710049, China
[b] Canadian Nuclear Safety Commission, 280 Slater Street, Ottawa, ON, K1P 5S9, Canada

ARTICLE INFO

Article history:
Received 2 December 2015
Received in revised form 4 November 2016
Accepted 6 November 2016
Available online 12 November 2016

Keywords:
VNM
Heterogeneous
Control rod cusping effect
MSR
Pin-by-pin
PWR

ABSTRACT

The Variational Nodal Method (VNM) is generalized for heterogeneous nodes and applied to four kinds of problems including Molten Salt Reactor (MSR) core problem with continuous cross section profile, Pressurized Water Reactor (PWR) control rod cusping effect problem, PWR whole-core pin-by-pin problem, and heterogeneous PWR core problem without fuel-coolant homogenization in each pin cell. Two approaches have been investigated for the treatment of the nodal heterogeneity in this paper. To concentrate on spatial heterogeneity, diffusion approximation was adopted for the angular variable in neutron transport equation. To provide demonstrative numerical results, the codes in this paper were developed in slab geometry. The first method, named as function expansion (FE) method, expands nodal flux by orthogonal polynomials and the nodal cross sections are also expressed as spatial depended functions. The second path, named as finite sub-element (FS) method, takes advantage of the finite-element method by dividing each node into numbers of homogeneous sub-elements and expanding nodal flux into the combination of linear sub-element trial functions. Numerical tests have been carried out to evaluate the ability of the two nodal (coarse-mesh) heterogeneous VNMs by comparing with the fine-mesh homogeneous VNM. It has been demonstrated that both heterogeneous approaches can handle heterogeneous nodes. The FE method is good at continuous-changing heterogeneity as in the MSR core problem, while the FS method is good at discontinuous-changing heterogeneity such as the PWR pin-by-pin problem and heterogeneous PWR core problem. For problems with only one or two discontinuity points such as the PWR control rod cusping effect problem, both of the two methods can catch the effect with high efficiency.

1. Introduction

Modern nodal methods play an important role in reactor core neutronics calculation due to its high computation efficiency and accuracy (Wagner and Koebke, 1983). However, traditional nodal methods usually require cross-section homogenization within each node which unavoidably introduces errors or reduces the computational efficiency in the following scenarios.

Firstly, in new reactor design such as Molten Salt Reactor (MSR), the fluid fuel is continuously flowing. Continuous temperature and nuclide density distributions result in continuous cross section distribution in space especially in axial direction. Volume- or approximate flux-volume-weighted homogenization scheme within each node is needed if traditional nodal methods are employed. However, if we adopt volume-weighted homogenization scheme for the nodes, it will introduce obvious error to the flux distribution. In addition, accurate flux distribution cannot be obtained even the approximate flux-volume-weighted homogenization scheme is employed. Some tests have been done in the 'Results' part of this paper and we can find the most effective way for traditional nodal methods to reduce the error caused by homogenization is adopting fine nodal mesh, which will reduce the computational efficiency unfortunately.

Secondly, in the Pressurized Water Reactor (PWR) core, control rods keep moving along the axial direction with a step size of about 2 cm, while the nodal size of neutronics simulation is usually about 20 cm. It is common to have one or more control rods partially inserted into the corresponding nodes. In this case, a single node would consist of different materials with different macroscopic cross sections within the framework of the traditional two-step simulation method. The numerically simulated curve of control rod worth is not even a smooth curve but with a lot of wiggles. It is the so-called control rod cusping effect. Since 1980s, many

* Corresponding author.
E-mail address: yunzhao@mail.xjtu.edu.cn (Y. Li).

http://dx.doi.org/10.1016/j.anucene.2016.11.007
0306-4549/

methods have been investigated to eliminate it, such as flux-volume-weighted method (Yamamoto, 2004; Dall'Osso, 2002) and adaptive mesh method (Zhang, 2014). The former has to obtain an approximated flux distribution, while the later has to regenerate the spatial mesh after each control rod movement to avoid the appearance of heterogeneous nodes.

Thirdly, traditional PWR core computation employs two-step scheme: lattice calculation to provide assembly-homogenized cross sections, then core diffusion calculation and pin-power reconstruction to provide pin-power profile within the core. To reduce the error introduced by assembly homogenization and pin-power reconstruction, the following pin-by-pin scheme has caught the concentration: assembly calculation with pin-cell homogenization and then whole-core pin-by-pin calculation. Several pin-by-pin calculation codes have been developed, such as SCOPE2 (Tatsumi and Yamamoto, 2003) and EFEN (Li et al., 2014). However, the whole-core pin-by-pin problem consists of millions of meshes. Computational efficiency becomes one of main problems in whole-core pin-by-pin calculation. For example, a PWR can be divided into 10 million spatial meshes. Together with the SP_3 approximation and 4 energy groups, the calculation time is about 24 h for a single CPU (Yang et al., 2014) if there is no acceleration.

Fourthly, in recent years, High-Fidelity computing aims to carry out whole-core heterogeneous simulations with homogenization fully eliminated. In High-Fidelity computing of PWR, the heterogeneity within each pin-cell requires an extremely refined mesh which leads to the total number of spatial meshes becoming billions. The increase of spatial meshes does not only increase the number of unknowns, but also slows down the convergence. In this case, the convergence can be significantly improved if a heterogeneous coarse-mesh nodal method can be employed to replace the fine mesh methods.

To overcome difficulties from the above four scenarios, traditional homogeneous nodal methods are expected to be generalized into heterogeneous nodal methods to maintain the computing efficiency with high accuracy. Among those homogeneous nodal methods, Variational Nodal Method (Palmiotti et al., 1995) (VNM) is chosen due to its advantages (Lawrence, 1986; Wagner, 1989; Li et al., 2015) compared with the others. VNM is based on a functional for even-parity transport equation and the nodes are coupled together by odd-parity Lagrange multipliers. Response matrices are obtained by using a Ritz procedure and the flux, current and source are expanded by orthogonal polynomials. The exclusion of the transverse integration technique in VNM guarantees its advantages in accuracy.

Fanning and Palmiotti (Fanning and Palmiotti, 1997) developed a heterogeneous nodal method based on VNM for piece-wise constant heterogeneous nodes. The even- and odd-parity fluxes are expanded by polynomials. Throughout the derivation, the functional for the heterogeneous node is obtained which has the same form as that in homogeneous VNM. To calculate the response matrices, the heterogeneous node is divided into a number of homogeneous elements and then the integrals over the node are divided into a set of homogeneous integrals. This method has high efficiency with low expansion order. However, when the configuration and material is complicated within the heterogeneous node, the flux will change sharply in space. As the flux is expanded by polynomials over the entire node in this method, it's difficult for it to describe the flux distribution with sharp gradient accurately over the node. Smith (Smith et al., 2003) developed another heterogeneous Variational Nodal Method also for piece-wise constant heterogeneous nodes. It divides each node into sub-elements in which the cross sections are constants, and expands the flux by finite trial functions in space and spherical or simplified spherical harmonics in angle. In this method, high-order angular approximation is required to obtain accurate results in the problems with sharp flux gradient throughout the geometry, while the results are less sensitive to the refinement of the sub-elements. The main disadvantage of this method is the low computational efficiency when high spherical harmonics expansion order is adopted. Another heterogeneous nodal method for solving diffusion equation was developed by Makoto Tsuiki (Tsuiki and Hval, 2002). The most distinctive feature of this method is that the flux in a node is expanded into a set of functions which are numerically obtained by single-assembly calculations without assembly homogenization. Highly accurate results can be obtained because the assembly heterogeneous effect is taken into account in the single-assembly calculation. Besides, the accuracy of this method can be improved simply by increasing the order of expansion. However, computing the numerical expansion functions becomes an additional burden of the method.

This paper mainly concentrates on the spatial distribution of the flux and power affected by the heterogeneous node with diffusion approximation adopted. To assess the performances of different methods for different problems, we choose the one-dimensional (1D) slab geometry. In this paper, two approaches are investigated for the treatment of the nodal heterogeneity. In function expansion (FE) method, the flux is expanded into the sum of polynomials and the cross section is also expressed as a function of space. Additionally, unlike the method developed by Fanning and Palmiotti, the heterogeneous nodes needn't to be divided into homogeneous elements which means this method can treat both continuous and piecewise continuous cross section distribution. The finite sub-element (FS) method employs finite-element basis functions to expand flux in each node. In this method, the heterogeneous node should be divided into homogeneous sub-elements.

The rest of this paper is organized as following. In Section 2, the theories of two heterogeneous VNMs including the FE method and the FS method are introduced in 1D slab geometry for neutron-diffusion equation. In Section 3, the two methods are applied to the four kinds of problems: MSR core problem, PWR control rod cusping effect problem, PWR pin-by-pin problem and heterogeneous PWR core problem. The capabilities and limitations of these two methods are then discussed.

2. Theory

This basic theory of homogeneous VNM is presented in Palmiotti et al. (1995) and Li et al. (2015) clearly. Based on this, Sections 2.1 and 2.2 introduce the treatments for heterogeneous nodes in FE method and FS method respectively. The following theory is derived in 1D slab geometry with diffusion approximation.

2.1. The function expansion heterogeneous Variational Nodal Method

To treat the heterogeneous nodes in FE method, the cross sections are assumed to be functions of space. Then the diffusion functional for each node can be written as

$$F_v[\Phi,J]=\int_v dV\left\{D(x)\left(\frac{d}{dx}\Phi(x)\right)^2+(\Sigma_t(x)-\Sigma_s(x))\Phi(x)^2-2\Phi(x)S(x)\right\}+2\sum_{\gamma=1}^{2}\Phi(x)J(x). \tag{1}$$

where Φ is the scalar flux ($cm^{-2}\cdot s^{-1}$); D is the diffusion coefficient (cm); Σ_t is the total cross section (cm^{-1}); Σ_s is the within-group scattering cross section (cm^{-1}); S is the source term ($cm^{-3}\cdot s^{-1}$) including isotropic scattering and fission; γ represents the surfaces

of the node and J_γ stands for the net current ($cm^{-2}\cdot s^{-1}$) on the surfaces of the node.

Different from homogeneous VNM, all the cross sections in Eq. (1) of a node are functions of the spatial variable. Therefore, an explicit description of the material structure of the heterogeneous node is allowed. The scalar flux and source in a node are then represented as:

$$\begin{cases} \Phi(x) = \sum_i \varphi_i f_i(x) \\ S(x) = \sum_i s_i f_i(x) \end{cases}. \tag{2}$$

φ_i and s_i are the unknown coefficients and $f_i(x)$ are known orthogonal polynomials. Because of the heterogeneity in a node, the relationship between flux and source should be written as:

$$S(x) = \Sigma(x)\Phi(x) + \frac{1}{k}F(x)\Phi(x), \tag{3}$$

$$\Sigma(x)\Phi(x) = \sum_{g'\neq g}\Sigma^s_{gg'}(x)\Phi_{g'}(x), \tag{4}$$

$$\frac{1}{k}F(x)\Phi(x) = \sum_{g'}\frac{\chi_g}{k}\nu\Sigma_{f,g'}(x)\Phi_{g'}(x), \tag{5}$$

where k is the effective multiplication factor, $\chi_g\nu\Sigma_{f,g'}$ and $\Sigma^s_{gg'}$ are respectively the fission and scattering cross sections from energy group g' to g (cm^{-1}). The cross sections in this equation are not constants any more.

Substituting Eq. (2) into Eq. (3) leads to the relationship between the flux and source moments:

$$s_i = \int_v \left\{ \left(\Sigma(x) + \frac{1}{k}F(x)\right)\cdot(\varphi_1 f_1 + \varphi_2 f_2 + \cdots + \varphi_n f_n)\cdot f_i \right\} dx, \tag{6}$$

which is more complicated than that in homogeneous VNM.

Substituting Eq. (2) into the functional, Eq. (1), yields the reduced functional:

$$F_v[\boldsymbol{\varphi},\boldsymbol{j}] = \boldsymbol{\varphi}^T\boldsymbol{A}\boldsymbol{\varphi} - 2\boldsymbol{\varphi}^T\boldsymbol{s} + 2\boldsymbol{\varphi}^T\boldsymbol{M}\boldsymbol{j}, \tag{7}$$

where $\boldsymbol{\varphi}$, $\boldsymbol{s}$ and $\boldsymbol{j}$ are vectors constructed by the expansion moments of the flux, the source inside a node and the net current on the surface of a node. The matrices$\boldsymbol{A}$ and $\boldsymbol{M}$ is written as

$$A_{ii'} = \int_v \left\{ D(x)\cdot\frac{df_i(x)}{dx}\cdot\frac{df_{i'}(x)}{dx} + (\Sigma_t(x) - \Sigma_s(x))f_i(x)f_{i'}(x) \right\} dx, \tag{8}$$

$$M_{i\gamma} = f_i(x)|_{x=x_\gamma}. \tag{9}$$

By comparing the homogeneous and heterogeneous VNM formulas, it can find that the differences between them locates in the source construction in Eq. (6) and the formulation of matrix $\boldsymbol{A}$. If the spatial depended cross section has a rational representation, we can obtain an analytic solution of the integrations in Eq. (6) and Eq. (8); otherwise we have to obtain the numerical results of the integrations. Once we obtain the response matrix $\boldsymbol{A}$, all the following derivation are the same as homogeneous VNM.

2.2. The finite sub-element heterogeneous Variational Nodal Method

To consider the nodal heterogeneity, each node is further divided into a set of homogeneous sub-regions named sub-elements. The nodal functional is now written as a superposition of sub-element functional:

$$F_v[\Phi,J] = \sum_e F_e[\Phi_e,J], \tag{10}$$

where the element functional is written as:

$$F_e[\Phi_e,J] = \int_e dV\left\{ D_e\left(\frac{d}{dx}\Phi_e(x)\right)^2 + (\Sigma_{t,e} - \Sigma_{s,e})\Phi_e(x)^2 - 2\Phi_e(x)S_e(x) \right\} + 2\sum_{\gamma=1}^{2}\Phi_e(x)J(x). \tag{11}$$

We expand the flux and source in a node as:

$$\begin{cases} \Phi(x) = \sum_i \varphi_i l_i(x) \\ S(x) = \sum_i s_i l_i(x) \end{cases}. \tag{12}$$

Here, the expansion functions $l_i(x)$ are linear finite-element trial functions. Because net current is continuous across sub-element interfaces, the surface term in Eq. (11) only appears at the nodal interfaces.

In one dimension, the flux and source in element e are given as:

$$\begin{cases} \Phi_e(x) = \varphi_{e-}l_{e-}(x) + \varphi_{e+}l_{e+}(x) \\ S_e(x) = s_{e-}l_{e-}(x) + s_{e+}l_{e+}(x) \end{cases}, \quad x\in e, \tag{13}$$

where $e-$ and $e+$ respectively stands for the left and right sides of the element e. For the cross sections in each element are unique, the relationship between flux and source moments is written as:

$$\begin{cases} s_{e-} = \left(\Sigma_e + \frac{1}{k}\nu\Sigma_{f,e}\right)\varphi_{e-} \\ s_{e+} = \left(\Sigma_e + \frac{1}{k}\nu\Sigma_{f,e}\right)\varphi_{e+} \end{cases} \tag{14}$$

Substituting Eq. (13) into the element functional in Eq. (11) yields the reduced functional:

$$F_e[\boldsymbol{\varphi},\boldsymbol{j}] = \boldsymbol{\varphi}_e^T\boldsymbol{A}_e\boldsymbol{\varphi}_e - 2\boldsymbol{\varphi}_e^T\boldsymbol{F}_e\boldsymbol{s}_e + 2\boldsymbol{\varphi}_e^T\boldsymbol{M}_e\boldsymbol{j}, \tag{15}$$

where

$$A_{e,ii'} = \int_e \left\{ D_e\cdot\frac{dl_i(x)}{dx}\cdot\frac{dl_{i'}(x)}{dx} + (\Sigma_{t,e} - \Sigma_{s,e})l_i(x)l_{i'}(x) \right\} dx, \tag{16}$$

$$F_{e,ii'} = \int_e l_i(x)l_{i'}(x)dx, \tag{17}$$

$$M_{e,i\gamma} = l_i(x)|_{x=x_\gamma}. \tag{18}$$

We can find that the nodal expansion coefficients vector consist of the expansion coefficients of all the elements in the node. Thus, to obtain the nodal functional, we should map the element trial function coefficients to the nodal expansion coefficients. This can be easily achieved with a Boolean transformation matrix Ξ_e which provides the location information of element trial function coefficients in the nodal coefficient vector and ensures the continuity across element interfaces:

$$\boldsymbol{\varphi}_e = \Xi_e\boldsymbol{\varphi}, \tag{19}$$

Substituting Eq. (19) into Eq. (15), and then substituting Eq. (15) into Eq. (10) leads to the nodal functional:

$$F_v[\boldsymbol{\varphi},\boldsymbol{j}] = \boldsymbol{\varphi}^T\boldsymbol{A}\boldsymbol{\varphi} - 2\boldsymbol{\varphi}^T\boldsymbol{s} + 2\boldsymbol{\varphi}^T\boldsymbol{M}\boldsymbol{j}, \tag{20}$$

where

$$\boldsymbol{A} = \sum_e \Xi_e^T\boldsymbol{A}_e\Xi_e, \tag{21}$$

$$\boldsymbol{s} = \sum_e \Xi_e^T\boldsymbol{F}_e\boldsymbol{s}_e, \tag{22}$$

$$\boldsymbol{M} = \sum_e \Xi_e^T\boldsymbol{M}_e. \tag{23}$$

Once the reduced nodal functional is obtained, the following procedure is as the same as the homogeneous VNM. However, different from the FE method, the FS method requires dividing the nodes into homogeneous elements, so it is unable to treat the nodes with continuous-changing cross sections.

3. Results

Two computer codes, Violet-Hom1D and Violet-Het1D, have been developed to treat respectively 1D homogeneous and heterogeneous node problems with multigroup macroscopic cross sections. Violet-Hom1D is based on traditional VNM with diffusion approximation. Two heterogeneous VNMs have been developed in Violet-Het1D based on the theory aforementioned. Four typical problems have been calculated to evaluate the methods and computer codes developed in this paper.

3.1. MSR application

The 1D MSR core is 4 m long with local coordinate origin located as the bottom. The vacuum boundary condition is applied to both the top and the bottom of the core and the distributions of macroscopic cross sections are described as linear functions:

$$\Sigma_a(x) = 0.084 - 0.004375x, \quad x \in [0,4]\text{m}, \tag{24}$$

$$\nu\Sigma_f(x) = 0.094 - 0.005x, \quad x \in [0,4]\text{m}, \tag{25}$$

$$\Sigma_s(x) = 1.035 - 0.075x, \quad x \in [0,4]\text{m}. \tag{26}$$

To measure the heterogeneity caused by the cross section gradient, we define a quantity:

$$M = k_\infty^b - k_\infty^t \tag{27}$$

where k_∞^b and k_∞^t are the infinite multiplication factors of the bottom and the top of this core. The more M is greater than 0, the more heterogeneous the core becomes. In this case, M equals to 0.0063. According to MSRE (Engel and Haubenreich, 1962) which designed by Oak Ridge National Laboratory, the inlet and outlet temperature of the fuel and graphite in the hottest channel is 910 K, 960 K and 915 K, 965 K respectively. The reactivity coefficients of salt temperature and graphite temperature are -8.5 pcm/K and -4.7 pcm/K (Delpech et al., 2003) when U235 is loaded. We can approximately calculate the value of M in the hottest channel in MSRE is about 0.0066. So the heterogeneity caused by cross section distribution in our design is reasonable.

The fine mesh calculation was performed by Violet-Hom1D. It divided the entire domain into 1920 homogeneous nodes with 3rd order polynomials expansion within each node. Other verified codes, EFEN (Yang et al., 2014) and a Monte Carlo (MC) code, were also applied with the same fine homogeneous regions to provide independent verification. Violet-Het1D with the FE method was used to calculate this problem. It divided the core into 4 nodes with linear cross section in each node and the flux was expanded by a 7th order polynomials. In comparison, Violet-Hom1D was also used to calculate this problem with the same 4 nodes and 7th order expansion. Besides, the homogenized cross sections of each node in Violet-Hom1D are obtained by volume-weighted scheme.

The same eigenvalue (k_{eff}) 1.11691 was obtained by the fine mesh calculation, EFEN and Violet-Het1D solutions. Violet-Hom1D obtained the k_{eff} of 1.11693. In addition, the k_{eff} of MC calculation is 1.11692 ± 0.00002. Actually, they had almost the same eigenvalue with the error less than 2 pcm. The flux and error distributions are shown in Fig. 1. It can be observed that solutions obtained by the fine mesh calculation, EFEN, MC code and Violet-Het1D seem to agree pretty well with each other, while the solution obtained by 4-node Violet-Hom1D shows obvious difference with others, especially at the flux peak. In MC solution, the standard deviation of the flux distribution along the core is less than 0.2% except at the top of the core. As the normalized flux become less than 0.01 at the top of the core (from 390 cm to 400 cm), the standard deviation is about 3% there. To measure the accuracy of the treatments for nodal linear cross sections, we should first discuss the error distribution compared with fine mesh calculation. We can find the error of the 4-node Violet-Hom1D solution is waving along the core in a larger range, the error at the peak of the flux distribution is 3.4% and the max error is −4.5%. In contrast, the error of Violet-Het1D is more stable, the error at the flux peak is around 0 and the max error is about 2.0% at the top of the core where the normalized flux is less than 0.01. When we take MC solution as the reference, we can find that Violet-Het1D still has better accuracy than Violet-Hom1D. What's more, their error distributions within the core (except boundaries) are almost as same as those when compared with fine mesh diffusion calculation: the error of Violet-Het1D is less than 1.5% and the error of Violet-Hom1D can be up to ±3.0%. Actually, it also proves that diffusion approximation does not introduce obvious error within the core as fine mesh diffusion solution agrees well with MC solution. However, at the two boundaries of the core which are applied with vacuum boundary condition, relatively larger error happens for both Violet-Het1D and Violet-Hom1D: −5.4%∼5.0% for Violet-Hom1D and −1.7%∼4.1% for Violet-Het1D. There are several reasons for the errors along boundaries: firstly, the normalized flux along the boundaries has small value (less than 0.01); secondly, the diffusion approximation in Violet-Het1D and Violet-Hom1D will certainly introduce some error near the vacuum boundaries; additionally, MC calculation also has relatively larger standard deviation there.

To further investigate the source of the error within the core, we analysis three main factors: expansion order, number of nodes and homogenization method. In the following analysis, we directly take the MC solution as the reference. Firstly, this paper varies the expansion orders both in Violet-Hom1D and Violet-Het1D with the number of nodes fixed. The errors at flux peak are shown in Fig. 2. We can find that when the expansion order is below 5, the error decreases with the increasing of expansion order. However, when the expansion order increases to higher than 5, the error becomes stable: the error of Violet-Het1D is about 0.2%; while the error of Violet-Hom1D is about 3.4%, much larger than that in Violet-Het1D. Therefore, increasing the expansion order obtains little improvement in the problem; it's not the main source of error in Violet-Hom1D.

Secondly, an additional comparison is made about the number of nodes. The expansion order is 7 in both Violet-Hom1D and Violet-Het1D. And also the errors at flux peak are shown in Fig. 3. We can find that increasing the number of nodes obtains obvious improvements for Violet-Hom1D. However, it requires more nodes in Violet-Hom1D than Violet-Het1D to reach the same accuracy. For example, when Violet-Het1D adopts 4 nodes, Violet-Hom1D should adopt about 16 nodes to obtain the solution with the same precision which will definitely reduce the computational efficiency.

Thirdly, to obtain the flux spectrum for the two nodes at the outer boundary, single node calculation with vacuum and reflective boundary conditions were carried out, while single node with reflective boundary conditions were done for the two nodes in the center of the core. We didn't consider the discontinuous factor in this case because when axial rehomogenization is carried out in engineering design, discontinuous factor is actually not taken into consideration. The approximate flux-volume-weighted homogenized cross sections are generated by:

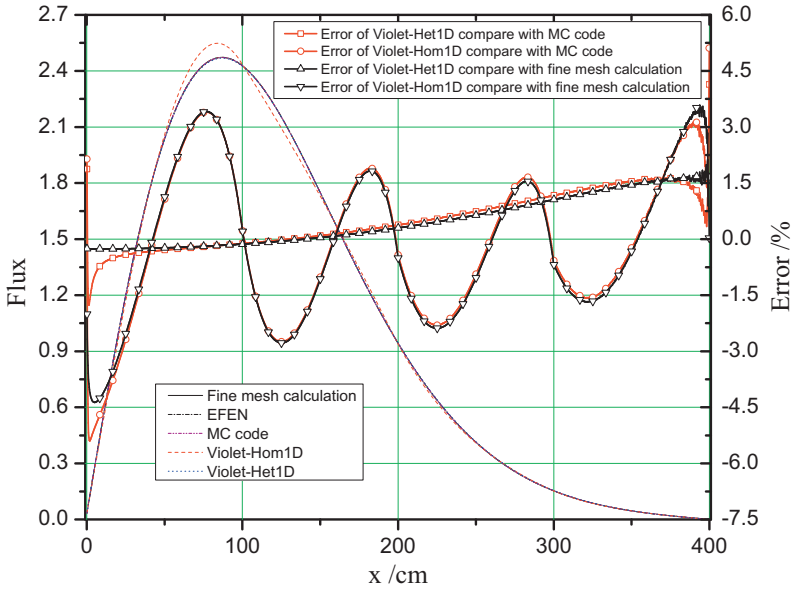

Fig. 1. Flux and relative error distributions with volume-weighted scheme in Violet-Hom1D.

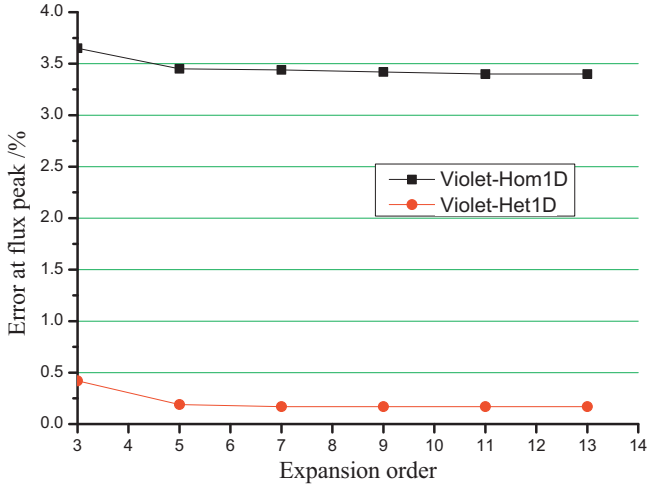

Fig. 2. Error at flux peak with different expansion orders.

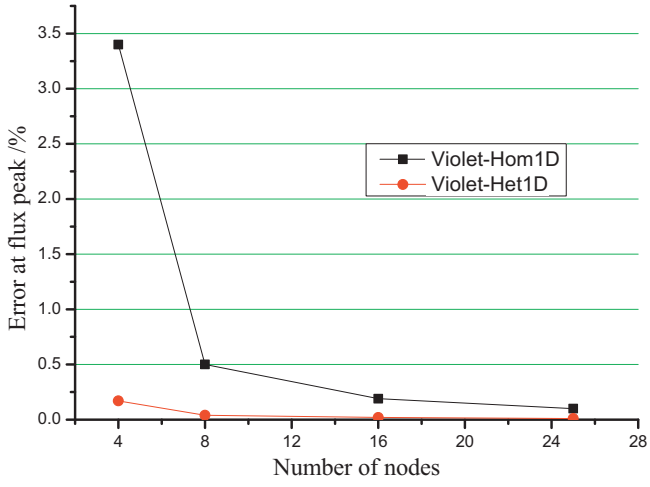

Fig. 3. Error at flux peak with different number of nodes.

$$\overline{\Sigma}_x = \frac{\int \Sigma_x(x)\phi(x)dx}{\int \phi(x)dx}. \tag{28}$$

The results are shown in Fig. 4. Compare with Fig. 1, we can find the flux peak fits better to the reference and the error is about 1.9%. However, the error of the rest part of the core increases, the error reaches 5–10% at the middle of the core. In a word, the solution is still not satisfactory even with the approximate flux-volume-weighted homogenization.

In summary, when homogeneous VNM is adopted to treat continuous cross section distributions in the MSR problem, the most effective way to reduce the error caused by homogenization is to employ fine nodal mesh. However, the increase number of nodal mesh will reduce the computational efficiency definitely. In contrast, the numerical results show that heterogeneous VNM is capable of obtaining accurate flux distribution without homogenizing the continuous cross sections in large-size nodes. In addition, the flux error of Violet-Hom1D increases with the heterogeneity of the core relatively, while the error of Violet-Het1D is almost fixed. To demonstrate this point, the paper listed the errors at the flux peak with respect to the heterogeneity of the core by using Violet-Het1D and Violet-Hom1D as indicated by Fig. 5.when M is in the range from 0 to 0.08, the errors of Violet-Het1D are always less than 0.5%, but the errors of Violet-Hom1D seem to increase approximate linearly with M.

3.2. Control rod cusping effect

Nodal methods have been widely used in PWR core design and safety analysis. Mostly, we take a whole assembly or a quarter of an assembly as one node and 10–20 cm per mesh in axial direction. The homogeneous cross sections in each node are provided by lattice calculation. Actually, control rods keep moving along the axial direction within the reactor core with a step size of about 2 cm, which may cause the appearance of nodes with partially inserted control rods. Unfortunately, almost all of the PWR lattice codes are in two-dimensional and thus cannot directly provide the homogenized cross section of the axially heterogeneous nodes. Actually, the homogenized cross sections of the nodes with partially inserted control rods are obtained by equivalent weighting methods (Si, 2006).

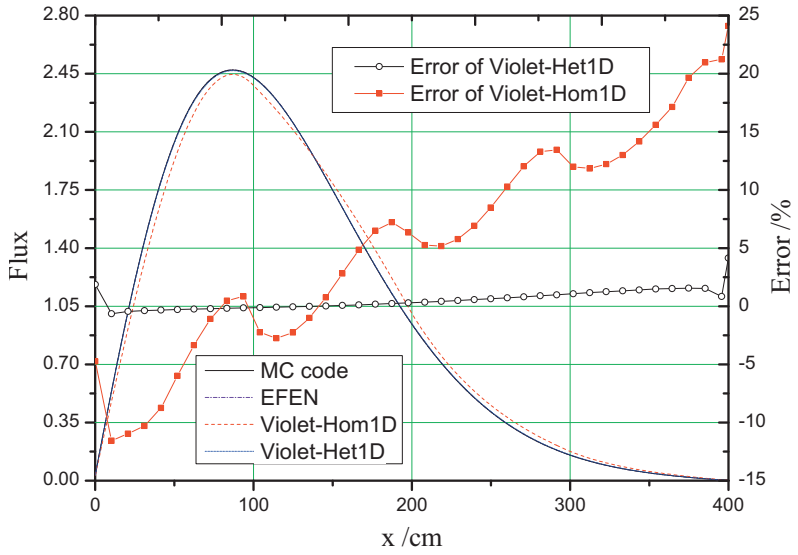

Fig. 4. Flux and relative error distributions with approximate flux-volume-weighted scheme in Violet-Hom1D.

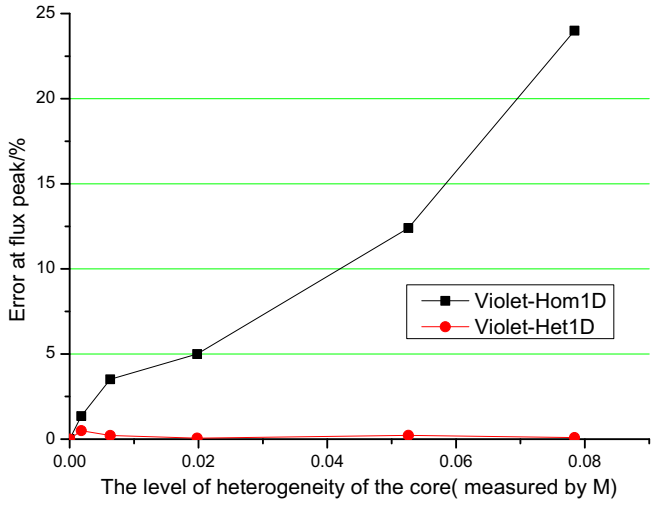

Fig. 5. Comparison of errors at flux peak with different level of heterogeneity.

In some early core-analysis codes, volume-weighted method is adopted, which is equivalent to the assumption of flat flux within the node. In fact, the insertion of control rods greatly affects the shape of flux distribution, especially the thermal flux. The flux is much depressed for the region with the control rods. As a result, it causes the numerically simulated curve of control rod differential worth different from the theoretically predicted shape. The numerically simulated curve of control rod worth is not even a smooth curve but with a lot of wiggles which introduced by directly volume-weighted schedule to obtain a constant macroscopic cross section. This phenomenon is the so-called control rod cusping effect which has negative effects on the core analysis, such as introducing extra errors in the analysis of some control-rod-initiated events and affecting on the calculation of axial power offset (AO).

Since the 1980s, many methods have been investigated to eliminate the control rod cusping effect which can be classified into three categories: approximate flux-volume-weighted method (Yamamoto, 2004), reconstructed axial flux-volume-weighted method (Dall'Osso, 2002) and adaptive mesh method (Zhang, 2014).

The approximate flux-volume-weighted method utilizes the average fluxes of the nodes with partially inserted control rods and the two adjacent nodes. If node k is partially inserted with control rod, nodes $k-1$ and $k+1$ are the two adjacent nodes. In addition, nodes $k-1$ and $k+1$ are the nodes without inserted control rods and with inserted control rods respectively. The average fluxes of the inserted section (R) and the non-inserted section (NR) of node k are approximated by:

$$\phi_{NR} = \frac{\Delta z_{k-1}\phi_{k-1} + (1-f_R)\Delta z_k \phi_k}{\Delta z_{k-1} + (1-f_R)\Delta z_k}, \tag{29}$$

$$\phi_R = \frac{\Delta z_{k+1}\phi_{k+1} + f_R \Delta z_k \phi_k}{\Delta z_{k+1} + f_R \Delta z_k}, \tag{30}$$

where Δz stands for the size of the node in axial direction and f_R is the insertion percentage of the control rod. Then the homogenized cross section of the node with inserted control rods is obtained by:

$$\overline{\Sigma}_x = \frac{(1-f_R)\Sigma_{NR,x}\phi_{NR} + f_R\Sigma_{R,x}\phi_R}{(1-f_R)\phi_{NR} + f_R\phi_R}. \tag{31}$$

This method is very efficient because it only utilizes the average fluxes of three adjacent nodes. However, the issue is its accuracy due to the accuracy of ϕ_R and ϕ_{NR} .

In reconstructed axial flux-volume-weighted method, the reconstruction procedure is carried out to obtain the flux distribution in the nodes with inserted control rods by using nodal surface flux and current. The homogenized cross section is then calculated by:

$$\overline{\Sigma}_x = \frac{\int_0^{\Delta z_k} \Sigma_x \phi dz}{\int_0^{\Delta z_k} \phi dz}. \tag{32}$$

Obviously, the accurate flux distribution improves the precision of the solution. However, the reconstruction of the axial flux decreases its efficiency relatively.

The adaptive mesh method doesn't adopt the flux-volume-weighted scheme to obtain the homogenized cross sections. It generates the meshes according to the position of control rods to ensure the bottoms of control rods aligned with the surfaces of the nodes. It avoids the heterogeneous nodes. However, problems arise from several aspects. First, it makes the core-analysis code more complicate for generating adaptive meshes. Second, it

increases the number of total nodes in the core which reduces the calculation efficiency. Third, if the bottoms of several control rods are very close in the axial direction, some layers of nodes would be very thin in the axial direction which may make it difficult for nodal method to converge.

In conclusion, approximate flux-volume-weighted method has high efficiency but low accuracy; reconstructed axial flux-volume-weighted method has high accuracy with relatively low efficiency; the adaptive mesh method avoids the control rod cusping effect by regenerating meshes, but it has some other problems as mentioned before. So is there a method that provides both high efficiency and accuracy without regenerating the meshes? Heterogeneous VNM is a good choice. It uses fixed meshes and treats the heterogeneous nodes directly without cross-section homogenization. It provides the accurate flux distribution in the nodes with inserted control rods.

We consider a 1D core with 4 m long. There are two types of material in the core: fuel with control rod fuel without control rod as shown in Fig. 6. The two-group homogeneous cross sections of the materials are listed in Table 1. The control rod moves along the axial direction with 2 cm each step. NECP-Cypress (Li et al., 2016) was adopted to obtain the reference solution of differential worth of the control rod. In this case, the core was divided into 200 nodes with the uniform mesh of 2 cm. Let the control rod move from the top to the bottom of the core. Then we utilized NECP-Cypress to calculate this problem every time the control rod took a step. To simulate a practical core calculation by using Violet-Hom1D, the entire core is divided to 20 nodes with each node 20 cm long. With the traditional volume-weighted method and 5th order flux expansion, the control rod cusping effect occurs as shown in Fig. 7. In contrast, Violet-Het1D explicitly describes the nodal heterogeneity. With the FE method, it uses 20 nodes and 5th order of expansion, while 20 nodes and 10 elements in each node for the FS method. As shown in Fig. 7, the solutions provided by Violet-Het1D fit the reference very well. It completely eliminates the control rod cusping effect and doesn't need any extra weighted scheme to obtain the homogeneous cross sections in the heterogeneous nodes.

Fig. 8 shows the comparison of power distribution when the control rod takes 105 steps (210 cm from the top of the core) down into the core. We can find from the error that when volume-weighted homogenization scheme is adopted within the heterogeneous node, the power of the part with control rod is higher than the reference while the power of the part without control rod is lower than the reference with the error of about 0.5%. So along with the control cusping effect, volume-weighted homogenization also affects the power distribution of the core which will further affect the calculation of AO. While, the power distribution obtained by Violet-Het1D agrees well to the reference, the maximum relative error of FE method is about 0.15% and the maximum error of FS method is 0.05%.

The computing time for the four schemes is shown in Table 2. We can find the FS method takes more time than the FE method mainly because the dimension of the response matrix $\boldsymbol{A}$ is 11×11 which is larger than 6×6 in the FE method. Violet-Het1D with the FE method takes a little more time than Violet-Hom1D in calculating the response matrix because of the nodal heterogeneity as shown in Eq. (8). The iteration time of Violet-Hom1D and Violet-Het1D with the FE method is the same with the same expansion order.

3.3. PWR Pin-by-pin problem

In order to evaluate Violet-Het1D's ability of treating complicated heterogeneity, we design an 1D PWR pin-by-pin problem respectively with pin-cell-homogenized macroscopic cross sections. The center symmetric configuration of the entire reactor core is shown in Fig. 9. Only half of the core is simulated during these calculations. The pin-by-pin assembly configurations are shown in Fig. 10. The single-group cross sections of this problem are listed in Table 3.

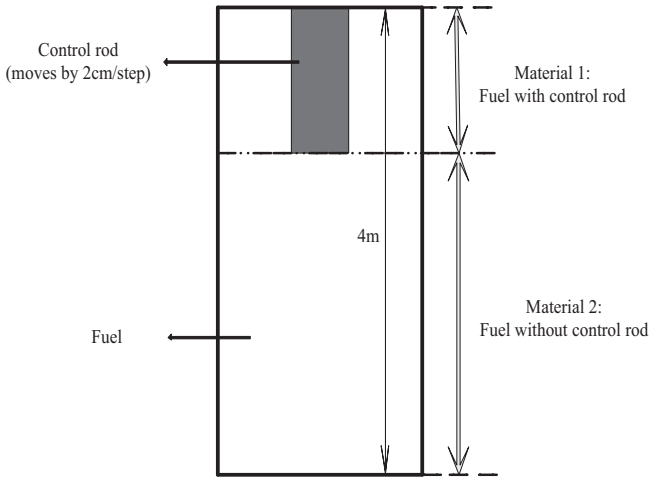

Fig. 6. Configuration of the one dimensional reactor core in the problem of control rod cusping effect.

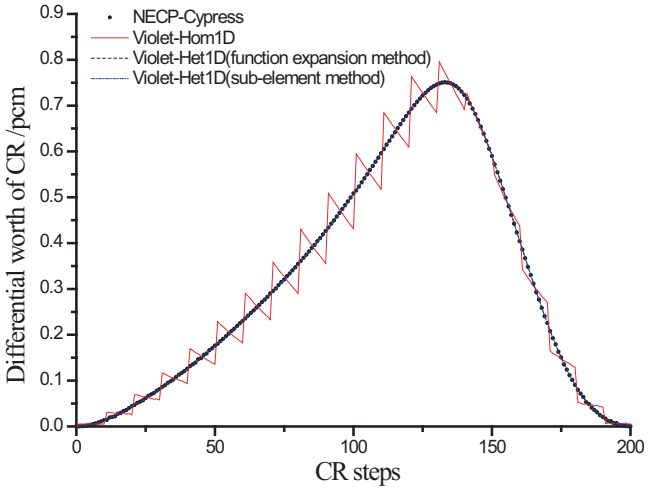

Fig. 7. Differential worth of control rod.

Table 1
The two-group homogeneous cross sections in the problem of control rod cusping effect.

Material	Energy group	D/cm	Σ_a/cm^{-1}	$\nu\Sigma_f$/cm^{-1}	$\Sigma_{s,12}$/cm^{-1}	χ
Fuel with control rod	1	6.62032	0.0	0.0	0.05035	1.0
	2	5.96837	0.05585	0.05400		0.0
Fuel without control rod	1	6.62032	0.0	0.0	0.05035	1.0
	2	6.06061	0.05500	0.05600		0.0

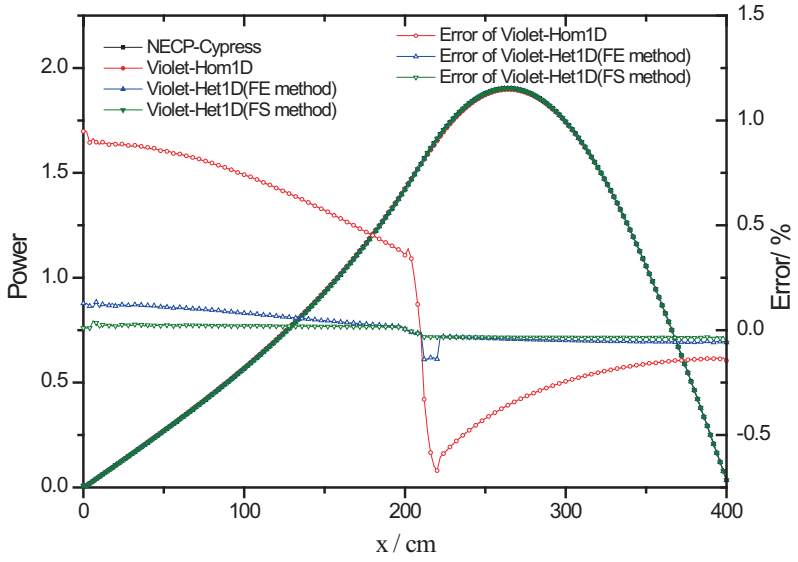

Fig. 8. Comparison of power distribution when the control rod takes 105 steps inside the core.

Table 2
Comparison of computing time of different calculation schemes in the control rod cusping effect case.

Scheme	Reference	Violet-Hom1D	Violet-Het1D (expansion method)	Violet-Het1D (sub-element method)
Time/s	366.2	22.0	27.6	43.6

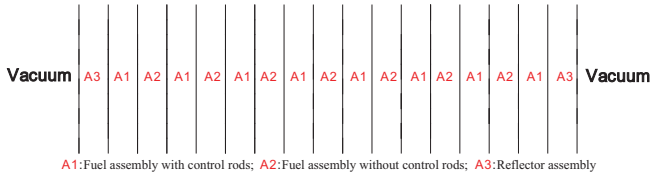

Fig. 9. Configuration of the one dimensional reactor core in the pin-by-pin problem (21.46 cm each assembly).

Ideally the neutron-transport equation should be solved in this problem. However, in order to evaluate Violet-Het1D's ability of treating spatial heterogeneity, the neutron-diffusion equation was solved for demonstration purpose. The fine mesh solution was obtained with Violet-Hom1D by taking each pin as a node (1.26 cm). It is sufficient to adopt 3th order expansion in this problem with small nodes. For Violet-Het1D, each assembly (21.42 cm) containing 17 pins was taken as a node. Additionally, a MC code was also adopted in this problem to make the comparison more adequate. The results of k_{eff} are shown in Table 4, while the flux and pin power distributions are shown in Figs. 11 and 12 respectively together with their relative errors comparing with both fine mesh and MC solutions. In MC solution, the standard deviation of the flux distribution in the fuel assemblies is less than 0.2%. However, in the reflector region where the normalized flux decreases from 0.01 to 0.001, the standard deviation increases from 2% to 10% there.

Firstly, we would like to analyze the accuracy of FE method in this problem. To evaluate the error introduced by the treatment for heterogeneous node, we should directly compare with fine mesh solution because they both solve the diffusion equation and the only difference between them is the nodal mesh. By comparing with fine mesh solution, we can find that when 7th order of polynomials is adopted in the FE method, the error of k_{eff} is −129 pcm. The maximum relative error of the flux and pin power

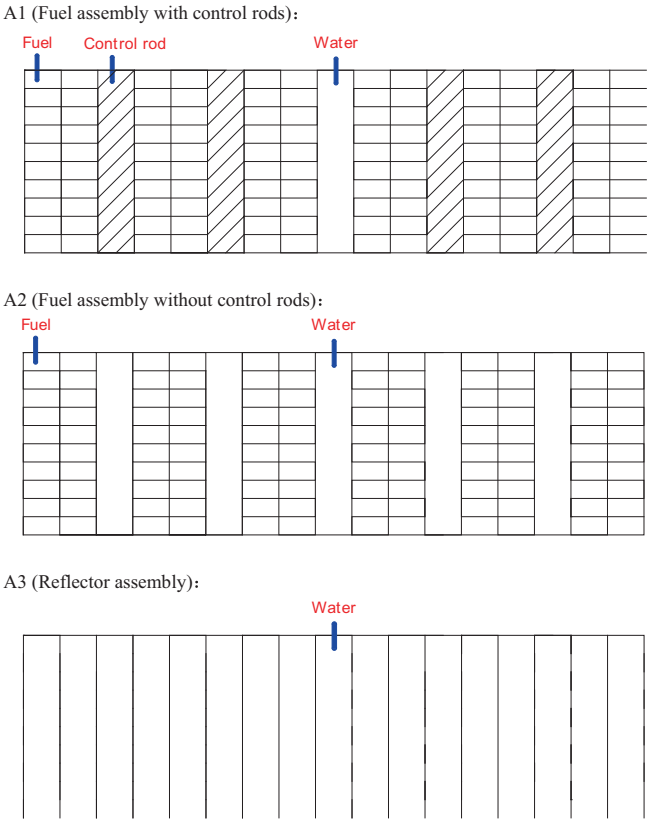

Fig. 10. Configuration of the pin-cell homogenized assemblies (1.26 cm each pin cell).

are about 20% which is unacceptable obviously. Further increasing the expansion order improves the accuracy of the solution. As shown in Table 4 and Fig. 11, when the expansion order is

Table 3
The single-group homogeneous cross sections of the pin-by-pin problem.

Material	D/cm	Σ_a/cm^{-1}	$\nu\Sigma_f$/cm^{-1}	Σ_s/cm^{-1}
Fuel	0.2979	0.0840	0.0940	1.0350
Control rod	0.3017	0.0609	0.0	1.0440
Water	0.2684	0.0066	0.0	1.2354

Table 4
The results of k_{eff} with different expansion order.

	MC code	Fine mesh calculation	Violet-Het1D-7	Violet-Het1D-20
k_{eff}	1.03881 ± 0.00002	1.03811	1.03682	1.03804

increased up to 20, the error of k_{eff} can be reduced to −7 pcm while the maximum relative error of the flux and pin power decreases to 3%. However, it becomes 5-time less efficient as indicated in Table 5. Although it reduces the number of iterations by requiring much less number of nodes, it has to cost more computing effort

Table 5
Comparison of node number and computing time with different expansion order.

	No. of nodes	Response matrices construction time/s	Iteration time /s	Total time /s
Fine mesh calculation	145	0.0	1.59	1.59
Violet-Het1D-7	9	0.02	0.15	0.17
Violet-Het1D-20	9	0.39	0.42	0.81

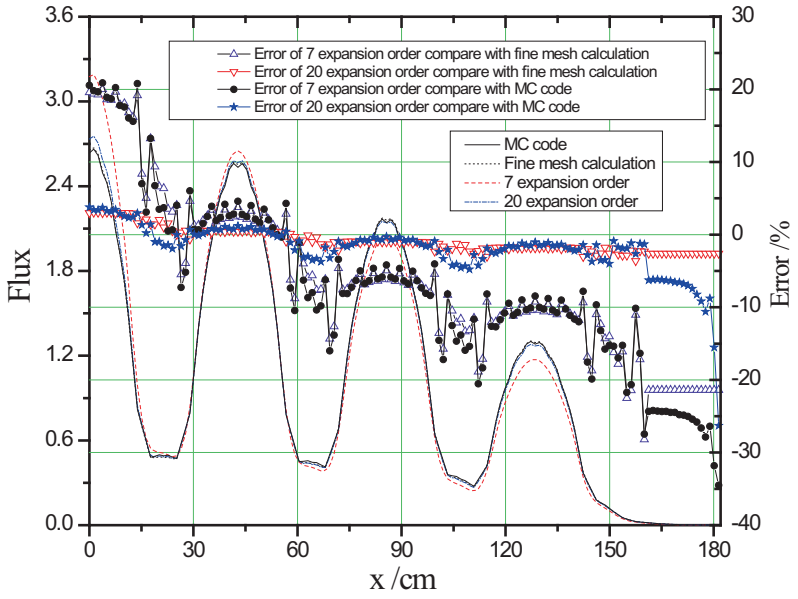

Fig. 11. Flux distribution comparison with different expansion order in the PWR pin-by-pin problem.

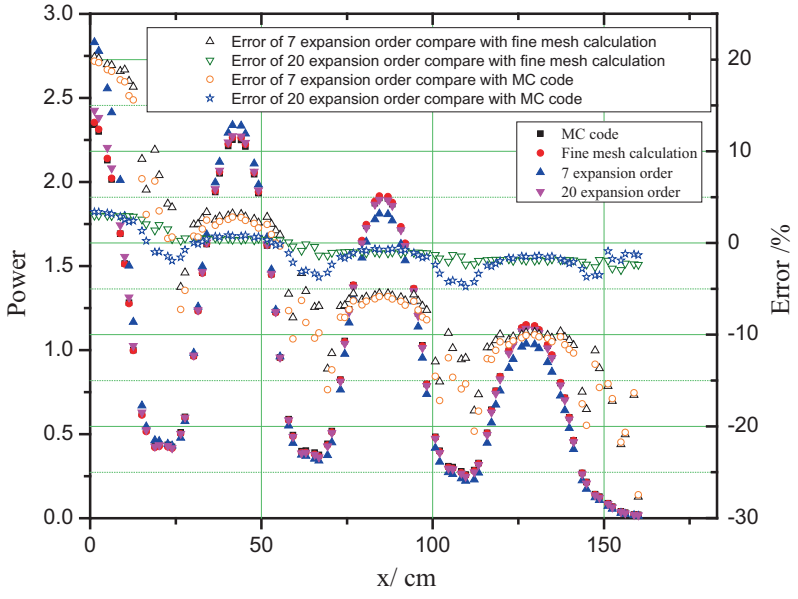

Fig. 12. Pin power distribution comparison with different expansion order in the PWR pin-by-pin problem.

within each iteration. Actually, FE method cannot achieve high accuracy in this problem because the large gradient of flux caused by strong discontinuity in cross section is difficult to be expanded by polynomials. If we compare the FE method with MC solution, the error is consisted of two parts: first, the error introduced in by the treatment of heterogeneous nodes which has been measured by comparing with fine mesh solution above; second, the error introduced by diffusion approximation in Violet-Het1D. As indicated in Table 4, the errors of k_{eff} are −199 pcm and −77 pcm respectively for 7th and 20th expansion order. Moreover, by comparing the error distributions in Figs. 11 and 12, we can find the two set of error distributions by comparing with fine mesh and MC solution respectively are very similar along the core except the reflector region which is close to the vacuum boundary and the pin cells which are close to control rods. It proves the second part of error mentioned above can be ignored except at the reflector region the pin cells around control rods. Actually, in the reflector region, the normalized average flux is smaller than 0.01 and it has relatively larger standard deviation. So if we pay more attention to the flux and power distribution in the fuel assemblies, we can find the error of the pin cells around control rods increases by 2–3% when comparing with MC code which means diffusion approximation has an error of 2–3% here.

The FS method was also tested to treat the pin-by-pin heterogeneity. Each assembly was taken as a node and two different numbers of elements in each node were calculated: 51 elements (3 elements in each pin) and 68 elements (4 elements in each pin). The results of k_{eff} are shown in Table 6 and the results of flux and pin power are shown in Figs. 13 and 14 respectively together with their relative errors comparing with both fine mesh and MC solutions. We can find from Table 6 that accurate k_{eff} can be obtained when compare with fine mesh calculation with the error less than 10 pcm; both fine mesh calculation and Violet-Het has about -70 pcm difference with MC code. As is shown in Figs. 13 and 14, the maximum relative error of flux and pin power is about 1.8% and 1.0% respectively for 51 and 68 elements in each node when compare with fine mesh solution. When it is compared with MC code, the maximum relative error is about 4.0% in the fuel assemblies. As this paper aims to evaluate the treatments for heterogeneity in FE and FS method, we can conclude that the FS method has more precise treatments than FE method because its solution shows better agreement with fine mesh solution. By comparing with MC solution, we can find that the error of pin-power around the control rods increases by 2% in both FE and FS method because of diffusion approximation.

The comparison of computing time is shown in Table 7. Firstly, the time for computing response matrices in FS method is much shorter than that in FE method with 20 expansion order (in Table 5) although the size of response matrices is much larger in FS method. The main reason is that the expansion functions are all linear functions which are easier to integrate. However, the large size of the response matrices will increase the time for iteration. When each node is divided into 68 elements, the dimension of the response matrix $\boldsymbol{A}$ is 69×69 and the time for iteration is 1.26 s, while the total computing time is 1.28 s which is just a little shorter than the computing time of the fine mesh calculation. However, when the problem becomes larger, the reducing number of nodes will obviously make the FS method more efficient. So in this problem, it is suitable to use the FS method with 68 elements in each node to obtain the results with relatively high efficiency and accuracy.

Table 6
The results of k_{eff} for the sub-element method in the PWR pin-by-pin problem.

	MC code	Fine mesh calculation	Violet-Het1D-51	Violet-Het1D-68
k_{eff}	1.03881 ± 0.00002	1.03811	1.03803	1. 03807

3.4. Heterogeneous PWR core problem

In the heterogeneous PWR core problem, the fuel rod and moderator are separated within each pin-cell, resulting in more complicated cross section distribution within each assembly. The configurations of the core and assemblies are shown as Figs. 9 and 10. In addition, the fuel pin and control rod pin consist of fuel

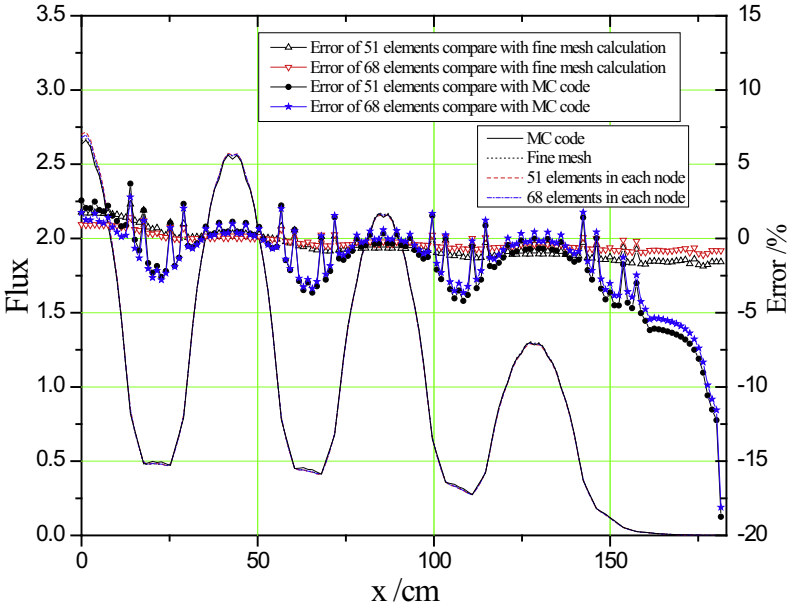

Fig. 13. Flux distribution comparison with different number of elements in each node in the PWR pin-by-pin problem.

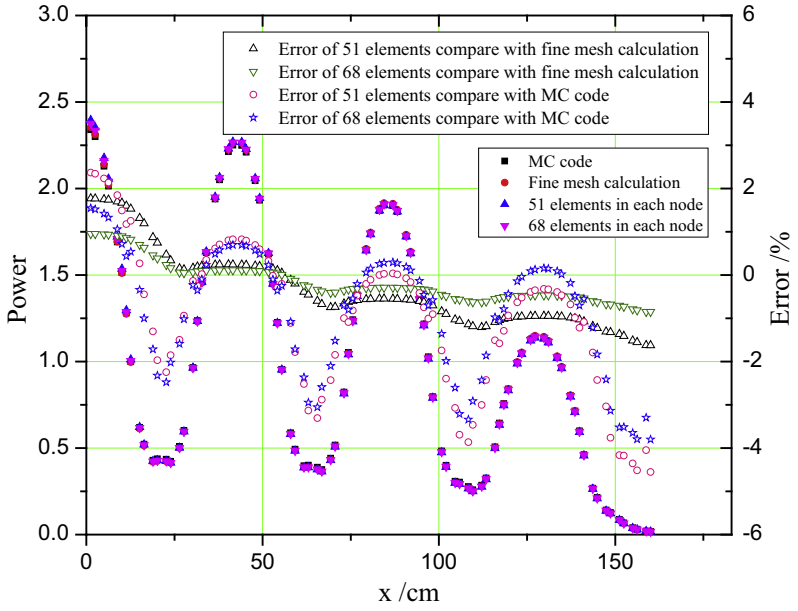

Fig. 14. Pin power distribution comparison with different number of elements in each node in the PWR pin-by-pin problem.

Table 7
Comparison of node number and computing time with different number of elements in each node in the PWR pin-by-pin problem.

	No. of nodes	Response matrices construction time/s	Iteration time /s	Total time/s
Fine mesh calculation	145	0.0	1.59	1.59
Violet-Het1D-51	9	0.01	0.87	0.88
Violet-Het1D-68	9	0.02	1.26	1.28

Table 8
The results of k_{eff} with different number of elements in each node in the heterogeneous PWR core problem.

	MC code	Fine mesh calculation	Violet-Het1D-68	Violet-Het1D-136
k_{eff}	1.00721 ± 0.00002	1.00632	1.00622	1.00630

rod and control rod in the middle and moderator surrounded it as shown in Fig. 15. Based on the analysis and conclusions in Section 3.3, we can find FE method is not capable of calculating accurate flux distribution in the problems with complicated configuration in the heterogeneous nodes. As this problem has more complex configuration within the assemblies than the pin-by-pin problem, only FS method is applied to it.

To obtain the solution of fine mesh calculation, we take 1/4 pin cell as a node (0.315 cm) in Violet-Hom1D and the expansion order is 3. A MC code is also employed in this problem to make the comparison. Additionally, the standard deviation of MC calculation of the flux distribution in the fuel assemblies is less than 0.2% and it increases from 2% to 12% in the reflector region as the normalized flux become very low. Then we calculate the problem using Violet-Het1D with the FS method. We take an assembly as one node and two different numbers of elements in each node are calculated: 68 elements (4 elements in each pin) and 136 elements (8 elements in each pin). Table 8 shows the results of k_{eff}: Violet-Het1D and fine mesh calculation obtain very similar eigenvalue with the difference of less than 10 pcm which proves the high accuracy of the treatment for heterogeneity in FS method. However, they both have a difference of about −90 pcm with MC code due to the diffusion approximation. Figs. 16 and 17 indicate that the flux and power distribution calculated by Violet-Het1D fits the fine mesh solution very well and the maximum relative error is about 1.5% and 0.5% when 68 and 136 elements are used in each assembly respectively. From the error distributions of flux and power comparing with MC code, we can find pin cells in the assemblies with control rods always have larger error. Fig. 17 indicates that most of the pin power errors are less than 2% while the error can be 3% when it's close to the reflector. As shown in Fig. 16, same as the previous problem, the flux distribution has larger error in the reflector due to its small order of magnitude (along with large standard deviation in MC calculation) and the diffusion approximation at vacuum boundary.

Table 9 lists the computing time of the FS method, which is only 10% and 25% of fine mesh calculation. Thus, the FS method obtains high efficiency in this problem while accurately treating the nodal heterogeneity.

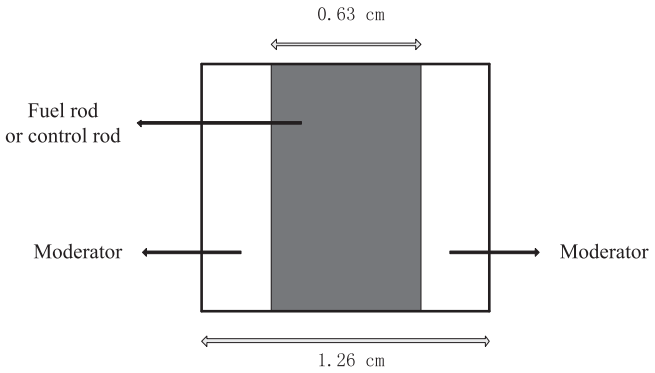

Fig. 15. Geometry information of the fuel pin and control rod pin in the heterogeneous PWR core problem.

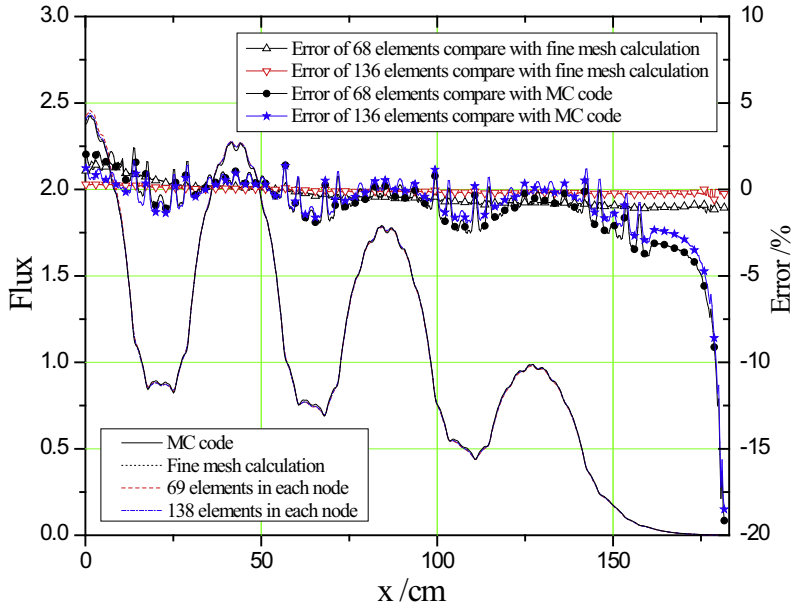

Fig. 16. Flux distribution comparison with different number of elements in each node in the heterogeneous PWR core problem.

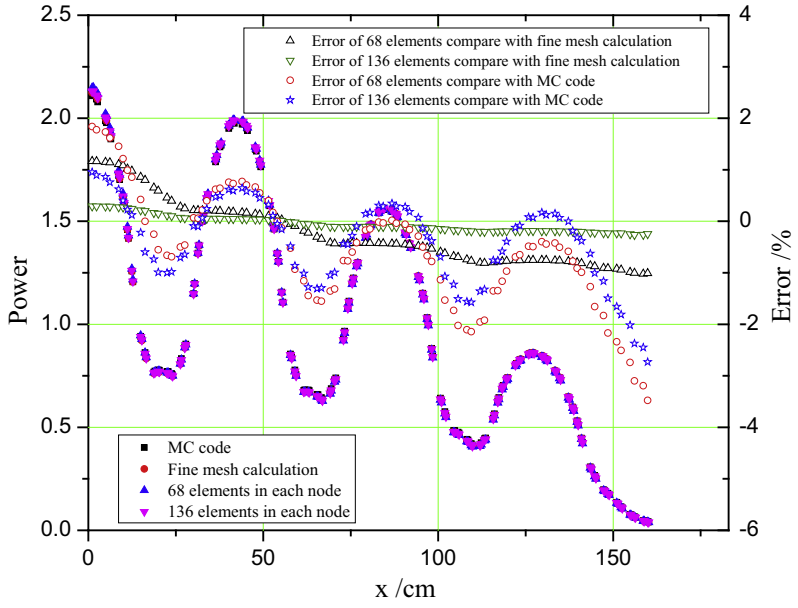

Fig. 17. Power distribution comparison with different number of elements in each node in the heterogeneous PWR core problem.

Table 9
Comparison of node number and computing time with different number of elements in each node in the heterogeneous PWR core problem.

	No. of nodes	Response matrices construction time/s	Iteration time/s	Total time/s
Fine mesh calculation	578	0.0	13.8	13.8
Violet-Het1D-68	9	0.02	1.11	1.13
Violet-Het1D-136	9	0.11	3.30	3.41

4. Conclusion

In this paper, we have introduced two generalized Variational Nodal Methods for treating heterogeneous nodes and the numerical results have shown the comparisons of the two methods in their applications to different problems. The function expansion (FE) method assumes the cross sections are functions of space and directly put these cross sections functions into the integration to compute the response matrices. This method can treat both continuous and piecewise continuous cross section distribution. The finite sub-element (FS) method breaks the heterogeneous node into small homogeneous elements and adopts linear finite-element trial functions as expansion functions. Codes Violet-Het1D and Violet-Hom1D are developed respectively based on heterogeneous and homogeneous VNM.

The FE method has been applied to a one dimensional Molten Salt Reactor (MSR) problem with spatially continuous cross sections. With the same expansion order and number of nodes, Violet-Het1D can get more precise solution than Violet-Hom1D. Additionally, the relative error at the flux peak obtained by

Violet-Hom1D seems to increase approximate linearly along with the heterogeneity of the core while the solution of Violet-Het1D maintains the high precision.

By employing the FE and FS methods to calculate the differential value of the control rod, we have found that both of them can eliminate the control rod cusping effect and obtain the accurate power distribution of the core.

By applying the FE method to the pin-by-pin problem, we have found that it is difficult to obtain the accurate solution even high expansion order is adopted because of the complicated configuration of the assembly. Besides, the time for computing response matrices increases rapidly with the expansion order. In contrast, the FS method can obtain the acceptably precise solution with the shorter time than that of the fine-mesh homogeneous VNM.

By applying the FS method to the heterogeneous Pressurized Water Reactor (PWR) core problem, we find that the FS method can obtain accurate results while maintain relatively high efficiency.

Considering the encouraging conclusions, these two heterogeneous nodal methods developed in this paper will be expanded to the neutron-transport equation and to three-dimensional geometry in the future.

Acknowledgment

This work was financially supported by the National Natural Science Foundation of China (11305123) – China.

References

Dall'Osso, A., Oct. 7–10, 2002. Reducing Rod Cusping Effect in Nodal Expansion Method Calculation, PHYSOR, Seoul, Korea.

Delpech, M., Dulla, S., Garzenne, C., Kophazi, J., et al., Nov., 2003. Benchmark of dynamic simulation tools for molten salt reactors. In: Nuclear Science and Technology: Meeting the Global Industrial and R&D Challenges of the 21st Century. New Orleans, United States.

Engel, J.R., Haubenreich, P.N., 1962. Temperatures in the MSRE Core During Steady-state Power Operation. Oak Ridge National Lab, Tenn.

Fanning, T.H., Palmiotti, G., 1997. Variational nodal method with heterogeneous nodes. Nucl. Sci. Eng. 127, 154–168.

Lawrence, R.D., 1986. Progress in nodal methods for the solution of the neutron diffusion and transport equations. Prog. Nucl. Energy 17, 271–301.

Li, Y., Cao, L., Yuan, X., Sept. 28–Oct. 3, 2014. High Order Source Approximation for the EFEN method. PHYSOR, Kyoto, Japan.

Li, Y., Wang, Y., Liang, B., Shen, W., 2015. Partitioned-matrix acceleration to the fission-source iteration of the variational nodal method. Prog. Nucl. Energy 85, 640–647.

Li, Y., Yang, W., Wu, H., Cao, L., Jun. 12–16, 2016. NECP-Cypress: development and benchmarking of a 3D PWR core analysis code. In: ANS Summer Meeting. New Orleans, United States.

Palmiotti, G., Lewis, E.E., Carrico, C.B., 1995. VARIANT: VARIational Anisotropic Nodal Transport for Multidimensional Cartesian and Hexagonal Geometry Calculation. Argonne National Laboratory, Argonne, IL USA. ANL-95/40.

Si, S., Jul. 1, 2006. Application research on the correction method of control rod cusping effect in three-dimensional core-analyze nodal code. In: Reactor Physics Conference (in Chinese). Harbin, China.

Smith, M.A., Tsoulfanidis, N., Lewis, E.E., Palmiotti, G., Taiwo, T.A., 2003. A finite subelement generalization of the variational nodal method. Nucl. Sci. Eng. 144, 36–46.

Tatsumi, M., Yamamoto, A., 2003. Advanced PWR core calculation based on multi-group nodal-transport method in three-dimensional pin-by-pin geometry. J. Nucl. Sci. Technol. 40 (6), 376–387.

Tsuiki, M., Hval, S., 2002. A variational nodal expansion method for the solution of multigroup neutron diffusion equations with heterogeneous nodes. Nucl. Sci. Eng. 141, 218–235.

Wagner, M.R., 1989. Three-dimensional nodal transport methods for hexagonal-z geometry. Nucl. Sci. Eng. 103, 377–391.

Wagner, M.R., Koebke, K., 1983. Progress in Nodal Reactor Analysis. In: Proc. Topl. Mtg. Advances in Reactor Computations, Salt Lake City, Utah, Mar. 28–31, 2, 941.

Yamamoto, A., 2004. A simple and efficient control rod cusping model for three-dimensional pin-by-pin core calculation. Nucl. Technol. 145.

Yang, W., Zheng, Y., Wu, H., Cao, L., Li, Y., 2014. High-performance whole core pin-by-pin calculation based on EFEN-SP_3 method. Nucl. Power Eng. (in Chinese) 35, 164–167.

Zhang, T., Jul. 7–11, 2014. Development of HEFT code system for the analysis of highly heterogeneous research reactors. In: Proceedings of the 2014 22nd International Conference on Nuclear Engineering, ICONE22. Prague, Czech Republic.